



Formic acid as the in-situ hydrogen source for catalytic reduction of nitrate in water by PdAg alloy nanoparticles supported on amine-functionalized SiO_2



Yajun Ding ^{a,b,1}, Wuzhu Sun ^{a,c,1}, Weiyi Yang ^a, Qi Li ^{a,*}

^a Environment Functional Materials Division, Shenyang National Laboratory for Materials Science, Institute of Metal Research, Chinese Academy of Sciences, Shenyang 110016, PR China

^b School of Materials Science and Engineering, University of Science and Technology of China, Hefei 230026, PR China

^c School of Materials Science and Engineering, Shandong University of Technology, Zibo 255000, PR China

ARTICLE INFO

Article history:

Received 23 June 2016

Received in revised form

18 September 2016

Accepted 18 October 2016

Available online 18 October 2016

Keywords:

Catalytic nitrate reduction
Formic acid
PdAg/ SiO_2 -NH₂ catalyst
—NH₂ surface modification
Electron transfer

ABSTRACT

Nitrate pollution in water is becoming a severe problem all over the world, and the catalytic reduction of nitrate by reducing agents had been considered as one of the most promising methods because it could convert nitrate to harmless nitrogen gas with a high efficiency. In this work, the PdAg/ SiO_2 -NH₂ catalyst was developed by firstly loading Pd onto —NH₂ surface-modified SiO_2 catalyst support, followed by a controlled surface reaction to load Ag and create PdAg alloy nanoparticles on SiO_2 -NH₂ catalyst support. For the first time, the PdAg/ SiO_2 -NH₂ catalyst was found to be able to effectively reduce nitrate with HCOOH as the reducing agent precursor. Its enhanced nitrate reduction performance could be attributed to the combination effects from the surface —NH₂ modification and the better electron transfer from Ag to Pd than from other metals due to their larger difference of work function, both of which were beneficial for the catalytic HCOOH decomposition to provide the in situ sources of the reducing agent of H₂ and buffer of CO₂ for the catalytic nitrate reduction process. To optimize the nitrate reduction performance of the PdAg/ SiO_2 -NH₂ catalyst, Ag content was carefully modulated and the Pd:Ag molar ratio of 1:0.5 was found to have the most efficient nitrate reduction capability.

© 2016 Elsevier B.V. All rights reserved.

1. Introduction

Nitrate pollution in water is becoming a severe problem all over the world due to its intensive release from both agricultural and industrial activities [1]. Excessive nitrate presence in water could cause water eutrophication under proper temperature conditions, resulting in the indiscriminate killing of aquatic organisms and the destruction of the local ecological equilibrium [2]. It could also cause series of damages to human health, including blue baby syndrome, high blood pressure, diabetes, liver damage, and various cancers [3]. Accordingly, regulatory agencies around the world had set up the maximum contaminant level (MCL) for nitrate in drinking water according to their domestic conditions to ensure the health of people. For example, the European Drinking Water Directive set its MCL for nitrate in drinking water at 50 mg/L [4], while a more strin-

gent standard was recommended by the World Health Organization at 25 mg/L [5]. To meet its drinking water standard, various processes had been developed to remove nitrate from water, including ion exchange [6], reverse osmosis [7], electrodialysis [8], photocatalytic reduction [9], catalytic reduction [10], and biological methods [11].

Among these techniques, catalytic reduction of nitrate by reducing agents had been considered as one of the most promising methods because it could convert nitrate to harmless nitrogen gas with a high efficiency [12]. Most catalysts for the nitrate reduction are composed of a noble metal and a promoter, in which the promoter reduces nitrate to nitrite by a redox process to start the catalytic process and nitrite is reduced by activated hydrogen on the noble metal [13]. Since the first successful demonstration of catalytic reduction of nitrate by Vorlop and Tacke [14], extensive research efforts have been made on this approach and hydrogen gas was used as the reducing agent in most of these works [15–21]. However, the use of H₂ in the catalytic reduction of nitrate may cause problems, especially when considering its potential for industrial applications. Due to its low solubility in water, large

* Corresponding author at: 72 Wenhua Road, Shenyang, Liaoning Province 110016, PR China.

E-mail addresses: qili@imr.ac.cn, qiliuic@gmail.com (Q. Li).

¹ These authors contributed equally to this work.

amounts of H₂ were wasted in this process and could be released into the environment, which only increased the cost of the operation but also posed a latent danger of explosion. In addition, the pH value of the treated water inevitably increased due to the formation of hydroxide ion during the catalytic reduction process with H₂ as the reducing agent [22], which could deteriorate the activity and selectivity of catalysts. Thus, CO₂ was needed to be bubbled into the solution with H₂ to stabilize its pH value at weakly acidic conditions, which increased the complexity of the apparatus and the operation.

Formic acid (HCOOH) is the simplest carboxylic acid, which is an important intermediate in chemical synthesis and could be produced as a by-product in the manufacture of other chemicals [23]. It could be decomposed into H₂ and CO₂ by noble metal catalysts [24–27], which makes it an in situ H₂ source for the enhancement of H₂ utilization efficiency in various reactions [28,29]. The simultaneously produced CO₂ could serve as the buffer to stabilize the solution pH in the catalytic reduction of nitrate [22,30]. Thus, a few attempts had been made to use HCOOH as the reducing agent precursor for the catalytic reduction of nitrate [9,22,30–32], in which Pd was used as the noble metal component and the promoter component examined were Cu, Sn, and In [31,13]. Till now, no report was available on the use of Ag as the promoter in the catalytic reduction of nitrate with HCOOH as the reducing agent precursor, while it had been reported that Pd/Ag could serve as a bimetal denitrification catalyst with H₂ as the reducing agent [33]. Furthermore, it had been reported that the existence of Ag could enhance the decomposition activity of Pd on HCOOH and the catalytic hydrogenation of Pd compared with other metals due to the larger difference of work function values between Pd and Ag [34,35]. Thus, it is of interest to examine the catalytic reduction of nitrate by Pd/Ag bimetal catalyst with HCOOH as the reducing agent precursor.

In this work, a PdAg/SiO₂-NH₂ catalyst was developed, and its catalytic nitrate reduction performance was examined with HCOOH as the reducing agent precursor. The surface of SiO₂ catalyst support was first modified by amine groups, which had been found to be beneficial for HCOOH decomposition [36–40]. PdAg alloy nanoparticles were loaded onto the SiO₂-NH₂ catalyst support by first loading Pd with a typical impregnation and subsequent reduction process [41], followed by a controlled surface reaction [42] to load Ag and create PdAg alloy. The PdAg/SiO₂-NH₂ catalyst was found to be able to effectively reduce nitrate with HCOOH as the reducing agent precursor for the first time. The catalytic nitrate reduction performance by the PdAg/SiO₂-NH₂ catalyst was found to be better in a closed reaction system than in an open reaction system. The surface –NH₂ modification of SiO₂ catalyst support largely enhanced its nitrate reduction efficiency, and PdAg alloy was superior to PdCu alloy as the catalyst for the nitrate reduction with HCOOH as the reducing agent precursor. The optimized Pd/Ag atomic ratio was found to be different between the catalytic HCOOH decomposition and the catalytic nitrate reduction.

2. Experimental

2.1. Materials and chemicals

All chemicals were of analytical grade and used without further purification. Silica gel was purchased from Qingdao Haiyang Chemical Corporation (Qingdao, P. R. China). (3-aminopropyl) triethoxysilane (H₂N(CH₂)₃Si(OC₂H₅)₃, APTS), palladium chloride (PdCl₂), silver nitrate (AgNO₃), copper chloride (CuCl₂), potassium borohydride (KBH₄), potassium nitrate (KNO₃), ethanol (C₂H₅OH), formic acid (HCOOH, 98%), sodium formate (HCOONa) were purchased from Sinopharm Chemical Reagent Corporation (Shanghai, PR China). Deionized water (18.2 MΩ) was obtained from a water

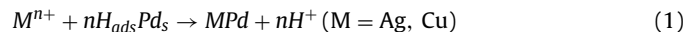
purification system. N₂ and CO₂ gases were purchased from Dalian Da Te gas Corp. Ltd. (Dalian, PR China), and H₂ gas was produced from a Guang Zheng hydrogen generator (Guang Zheng Analytical Instruments Corp. Ltd., Shenyang, PR China), and all the gases used in this work were of high purification (99.99%).

2.2. Surface modification of SiO₂ by –NH₂

SiO₂ sample was firstly dried in oven at 393 K for 2 h to remove physisorbed water. Next, 10 g of dried SiO₂ was put into a single-mouth flask containing 400 mL of dehydrated ethanol. The suspension was stirred for 0.5 h before the addition of 1 mL of APTS. Then, the flask was put into a water bath equipped with condenser pipe at 343 K and the suspension was stirred for 24 h before it was filtered with neutral filter paper. The obtained white powder was washed three times by dehydrated ethanol and dried in vacuum oven at 313 K overnight to obtain SiO₂ sample with –NH₂ surface modification.

2.3. Synthesis of PdAg/SiO₂-NH₂ and PdCu/SiO₂-NH₂ catalysts

Pd was firstly loaded onto SiO₂-NH₂ support by a typical impregnation and subsequent reduction process [41]. 400 mL of PdCl₂ aqueous solution was prepared by dissolving 13.36 mg of PdCl₂ and 17.61 mg of NaCl (the molar ratio of NaCl/PdCl₂ at ~4) into 400 mL of deionized water under ultrasonication for 30 min. Typically, 0.8 g of SiO₂-NH₂ support was added into 400 mL of PdCl₂ (13.36 mg) aqueous solution, and the suspension was stirred for 1 h before the addition of 40 mL of KBH₄ (1.6 g) aqueous solution. The suspension became black immediately and was stirred continuously for 0.5 h before it was filtered. After being dried in vacuum oven at 313 K overnight, Pd/SiO₂-NH₂ sample was obtained with ~1 wt% Pd. Then, Ag or Cu was further introduced by a controlled surface reaction method [42], in which the second metal was introduced through the reduction of the metal ion by hydrogen chemisorbed on Pd nanoparticles as described by Eq. (1):



2 g Pd/SiO₂-NH₂ was dispersed into 100 mL DI water under vigorous stirring and the suspension was bubbled with H₂ (200 mL/min) for 15 min. Aqueous solution of AgNO₃ or CuCl₂ with desired amount was then added into the suspension and it was continuously stirred for 1 h before it was filtered. After being dried in vacuum oven at 313 K overnight, PdAg/SiO₂-NH₂ or PdCu/SiO₂-NH₂ catalyst was obtained. A series of Pd:Ag atomic ratios of 1:1, 1:0.5, and 1:0.25 were obtained and the corresponding catalysts were named as PdAg1:1/SiO₂-NH₂, PdAg1:0.5/SiO₂-NH₂, and PdAg1:0.25/SiO₂-NH₂, respectively. Pd:Cu atomic ratio was set at 1:0.5. For comparison purpose, PdAg/SiO₂ catalyst was also prepared without –NH₂ surface modification.

2.4. Catalyst characterization

X-ray diffraction (XRD) patterns of catalyst samples were obtained from a D/MAX-2004 X-ray powder diffractometer (Rigaku Corporation, Tokyo, Japan) with Ni-filtered Cu ($\lambda = 0.15418 \text{ nm}$) radiation at 182 mA and 56 kV. X-ray photoelectron spectroscopy (XPS) measurements were conducted on an ESCALAB250 X-ray Photoelectron Spectrometer (Thermo Fisher Scientific Inc., Waltham, MA, U.S.A.) with an Al K anode (1486.6 eV photon energy, 300 W). The specific surface area and pore volume of catalyst samples were obtained with an Autosorb-1 Analyzer (Quantachrome Instruments, Boynton Beach, FL, U.S.A.). The microstructure of catalyst samples were observed by a FEI Tecnai F20 transmission electron microscope (FEI Ltd., Hillsboro, Oregon State, U.S.A.) operating at 200 kV. The contents of palladium, silver and copper in

these catalysts were obtained by an inductively coupled plasma optical emission spectrometer (Varian 720-ES, Varian, U.S.A.), and the samples were completely dissolved in the mixture aqueous solution of HNO_3/HCl (1/3 v/v) by ultrasonication and gentle heating. The existence of $-\text{NH}_2$ group on SiO_2 support was verified by the Fourier transform infrared spectroscopy (FTIR, NICOLET 6700 FTIR (Thermo Scientific, U.S.A.)), and the samples were prepared by grinding with KBr at a fixed ratio (1%). UV-vis spectra of catalyst samples were observed by a JASCO V-770 spectrophotometer (JASCO Ltd., Japan).

2.5. Catalytic reduction of nitrate experiments

All the catalytic nitrate reduction experiments were conducted in a 250 mL single-mouth glass flask with two glass pipes in the water bath at 298 K. In a typical setup, 0.4 g catalyst sample was loaded into the flask with 178 mL deionized water under vigorously stirring, and the suspension was bubbled by CO_2 (200 mL/min) for 15 min. Then, 22 mL of the mixture of 20 mL KNO_3 solution (1 g NO_3^-/L) and 2 mL $\text{HCOOH}/\text{HCOONa}$ solution (0.8 M: 0.4 M) was added into the flask to obtain the final NO_3^- concentration of $\sim 100 \text{ mg/L}$ and $\text{HCOOH}/\text{HCOONa}$ concentration of 8 mM/4 mM, and CO_2 bubbling was stopped immediately. Both the CO_2 bubbled and simultaneously produced during the HCOOH decomposition could serve as the buffer to stabilize the solution pH in the catalytic reduction of nitrate. The reaction was conducted either in open-mouth or close state. During the experiment, 5 mL suspension was withdrawn at the regular time interval. The catalyst was separated from the suspension by filtration, and the clear solution was used to determine concentrations of NH_4^+ , NO_3^- , NO_2^- , and HCOO^- by the ion chromatograph (Dionex ICS 1100 Ion Chromatography with a conductivity cell). The NH_4^+ concentration was determined by Dionex CS12A column with 20 mmol/L of methanesulfonic acid as the effluent, while the concentrations of NO_3^- , NO_2^- , and HCOO^- were determined by Dionex AS-22 column with 1.4 mmol/L bicarbonate and 4.2 mmol/L carbonate buffer solution as the effluent. The initial nitrate reduction rate was calculated with the change of NO_3^- concentration in the initial 10 min by Eq. (2):

$$\frac{100 \text{ mg/L} - [\text{NO}_3^-]_{10 \text{ min}}}{10 \text{ min} \times 0.4 \text{ g}} \times 0.2 \text{ L} \quad (2)$$

The nitrate conversion ($X_{\text{NO}_3^-}$) used to evaluate the catalyst activity and the selectivity of nitrate converted to NH_4^+ ($S_{\text{NH}_4^+}$) was calculated by Eqs. (3) and (4) respectively:

$$X_{\text{NO}_3^-} = \frac{C_{\text{NO}_3^-_{3t}} - C_{\text{NO}_3^-_{3i}}}{C_{\text{NO}_3^-_{3i}}} \quad (3)$$

$$S_{\text{NH}_4^+} = \frac{n_{\text{NH}_4^+_{4t}}}{n_{\text{NO}_3^-_{3i}} - n_{\text{NO}_3^-_{3t}} - n_{\text{NO}_2^-_{2t}}} \quad (4)$$

3. Results and discussion

3.1. Structure, morphology and composition of $\text{PdAg/SiO}_2\text{-NH}_2$ catalysts

Fig. 1a compares the FTIR spectra of SiO_2 support before and after $-\text{NH}_2$ surface modification. Their spectra were generally alike, while two peaks occurred at 2984 cm^{-1} and 2937 cm^{-1} on the FTIR spectrum of SiO_2 support after $-\text{NH}_2$ surface modification which could be attributed to the C–H stretching of APTS. Thus, it suggested that APTS was successfully loaded onto SiO_2 support to modify its surface with $-\text{NH}_2$ [43]. Fig. 1b shows the XRD patterns of $\text{PdAg/SiO}_2\text{-NH}_2$ catalysts with different Pd:Ag molar ratios, and the XRD patterns of SiO_2 and $\text{SiO}_2\text{-NH}_2$ were shown in Fig.

S1 in the Supplementary material. For the $\text{Pd/SiO}_2\text{-NH}_2$ catalyst, a weak diffraction peak assigned to Pd (111) could be clearly identified at $2\theta \sim 40^\circ$ (JCPDS: 04-0783), which demonstrated that Pd was successfully loaded to $\text{SiO}_2\text{-NH}_2$ catalyst support through the synthesis process. For the $\text{Ag/SiO}_2\text{-NH}_2$ catalyst, a weak diffraction peak assigned to Ag (111) could be clearly identified at $2\theta \sim 38^\circ$ (JCPDS: 46-1043), which demonstrated that Ag could also be successfully loaded to $\text{SiO}_2\text{-NH}_2$ catalyst support through the synthesis process. For samples with both Pd and Ag loadings (Pd:Ag molar ratio at 1:0.25, 1:0.5, and 1:1), it was clear that only one weak diffraction peak at 2θ between $\sim 38^\circ$ and $\sim 40^\circ$ could be observed in their XRD diffraction patterns, and their peak position gradually shifted from $\sim 39.5^\circ$ to $\sim 39^\circ$ with the increase of Pd:Ag molar ratio from 1:0.25 to 1:1. This observation suggested that PdAg alloy was formed during the controlled surface reaction process to load Ag onto $\text{Pd/SiO}_2\text{-NH}_2$ catalyst [44,45].

The morphology and microstructure of loaded PdAg alloy catalyst on $\text{SiO}_2\text{-NH}_2$ catalyst support were examined by both STEM and TEM observations. Fig. 1c shows the Z-contrast image of $\text{PdAg1:0.5/SiO}_2\text{-NH}_2$ catalyst obtained by high angle annular dark field (HAADF) STEM technique, which demonstrated that highly-dispersed bright nanoparticles with relatively uniform size of several nm were embedded in relatively dark substrate. The insert image in Fig. 1c shows the energy dispersive X-ray analysis (EDS) spectrum collected from the bright nanoparticles, which clearly demonstrated the existence of Pd and Ag. While no Pd and Ag signals could be collected on the relatively dark substrate area. This observation (together with XRD analysis results) clearly demonstrated that loaded PdAg alloy catalyst existed as fine PdAg alloy nanoparticles well-dispersed on $\text{SiO}_2\text{-NH}_2$ catalyst support, which was beneficial for its catalytic performance. Fig. 1d shows the TEM image of $\text{PdAg1:0.5/SiO}_2\text{-NH}_2$ catalyst, which also clearly demonstrated that PdAg alloy nanoparticles with the size of several nm (dark color) were dispersed well on $\text{SiO}_2\text{-NH}_2$ catalyst support (lighter color). The insert particle size distribution image in Fig. 1d was determined by the professional image processing and analysis software of Image-Pro Plus 5.0 on over 10 TEM images by the quantitative statistical method. The insert HRTEM image in Fig. 1d shows one PdAg alloy nanoparticle, which verified its highly crystallized structure. One set of lattice planes could be clearly observed with the d -spacing at $\sim 0.23 \text{ nm}$, while the d -spacings of the (111) planes of fcc Pd phase and fcc Ag phase were 0.22 nm and 0.24 nm , respectively. Thus, the HRTEM observation provided another evidence that PdAg alloy was formed on $\text{SiO}_2\text{-NH}_2$ catalyst support and the observed set of lattice planes should be corresponded to the (111) plane of PdAg alloy phase. Fig. 1e compares the DR-UV-vis spectra of the $\text{Ag0.5 wt\%}/\text{SiO}_2\text{-NH}_2$ catalyst and the $\text{PdAg1:0.5/SiO}_2\text{-NH}_2$ catalyst. It showed clearly that the $\text{Ag0.5 wt\%}/\text{SiO}_2\text{-NH}_2$ catalyst had a strong surface plasmon resonance (SPR) band at $\sim 400 \text{ nm}$, while no such SPR band could be observed on the $\text{PdAg1:0.5/SiO}_2\text{-NH}_2$ catalyst. This observation was in accordance with the report by Bulut et al. and could be attributed to the alloying effect between Pd and Ag [46].

Fig. 2a shows the representative survey XPS spectrum of $\text{PdAg1:0.5/SiO}_2\text{-NH}_2$ catalyst, which clearly demonstrated the existence of Ag, Pd, Si, O, C, and N elements. Fig. 2b compares the high-resolution XPS scans over Ag 3d peaks of $\text{PdAg1:0.5/SiO}_2\text{-NH}_2$ catalyst and $\text{Ag0.5 wt\%}/\text{SiO}_2\text{-NH}_2$ catalyst. It demonstrated that the binding energy of Ag 3d peaks of $\text{PdAg1:0.5/SiO}_2\text{-NH}_2$ catalyst shifted towards larger values, compared to that of $\text{Ag/SiO}_2\text{-NH}_2$. Fig. 2c compares the high-resolution XPS scans over Pd 3d peaks of $\text{PdAg1:0.5/SiO}_2\text{-NH}_2$ catalyst and $\text{Pd1 wt\%}/\text{SiO}_2\text{-NH}_2$ catalyst. It demonstrated that the binding energy of Pd 3d peaks of $\text{PdAg1:0.5/SiO}_2\text{-NH}_2$ catalyst, however, shifted towards smaller values, compared to that of $\text{Pd/SiO}_2\text{-NH}_2$. The observed opposite binding energy shifting of Ag and Pd 3d peaks suggested that elec-

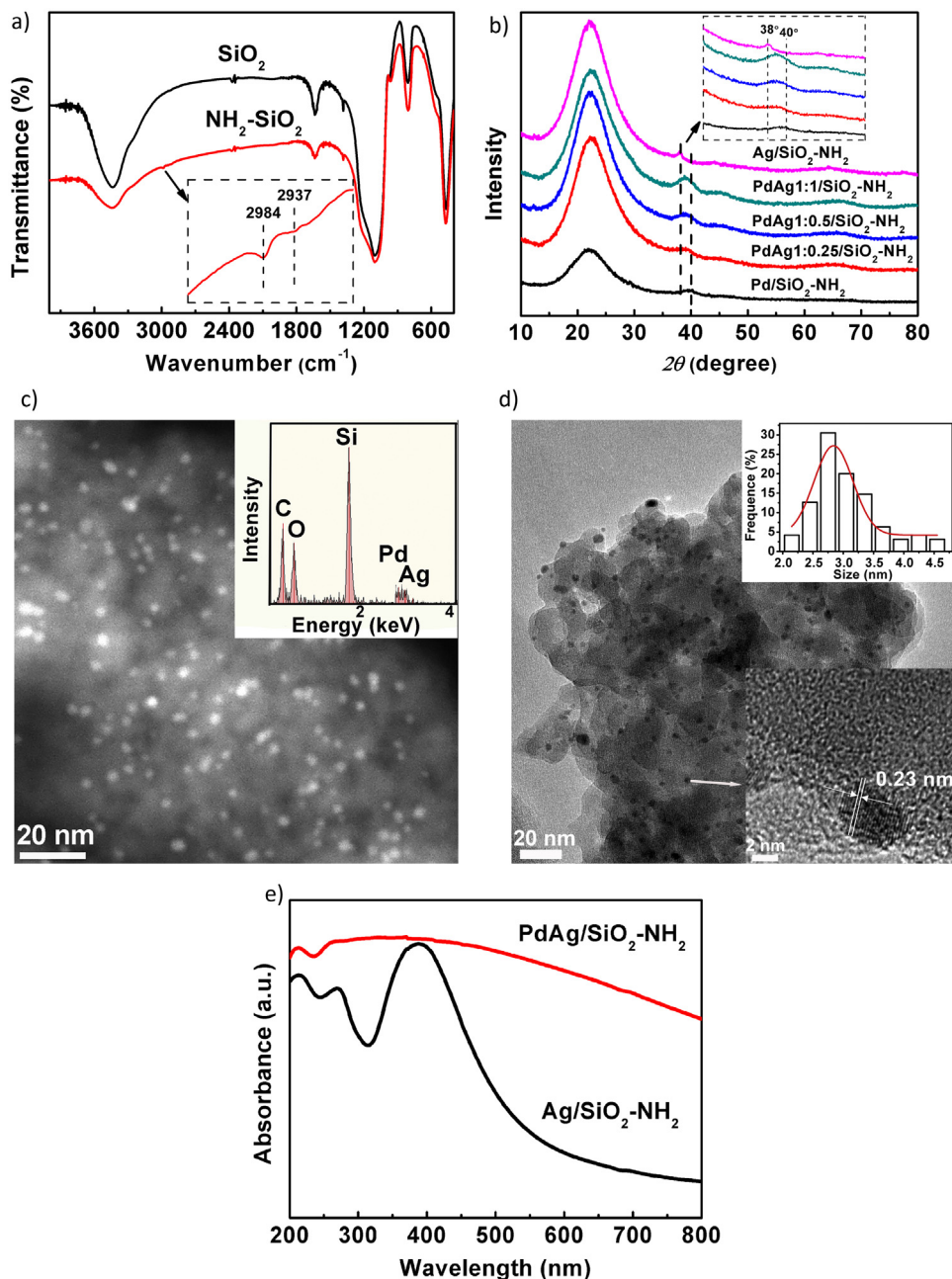


Fig 1. (a) FTIR spectra of SiO_2 support before and after $-\text{NH}_2$ surface modification. (b) XRD patterns of $\text{PdAg}/\text{SiO}_2\text{-NH}_2$ catalysts with different Pd:Ag molar ratios of 1:0.25, 1:0.5, and 1:1, compared with that of the $\text{Pd}/\text{SiO}_2\text{-NH}_2$ catalyst and the $\text{Ag}/\text{SiO}_2\text{-NH}_2$ catalyst. (c) Z-contrast image of $\text{PdAg1:0.5}/\text{SiO}_2\text{-NH}_2$ catalyst. (Note: Insert image in Fig. 1c shows the energy dispersive X-ray analysis (EDS) spectrum collected from the bright nanoparticles.) (d) TEM image of $\text{PdAg1:0.5}/\text{SiO}_2\text{-NH}_2$ catalyst (Note: Insert image in the top right of Fig. 1d shows the size distribution of PdAg alloy nanoparticle, and insert image in the bottom right of Fig. 1d shows the HRTEM observation on one PdAg alloy nanoparticle.) (e) DR-UV-vis spectra of the $0.5\text{ wt\%}/\text{SiO}_2\text{-NH}_2$ catalyst and the $\text{PdAg1:0.5}/\text{SiO}_2\text{-NH}_2$ catalyst.

trons were partially transferred from Ag to Pd in these PdAg alloy nanoparticles, which could be attributed to their different work functions for electron redistribution [34,47]. The transferring of electrons from Ag to Pd in $\text{PdAg}/\text{SiO}_2\text{-NH}_2$ catalyst could promote the catalytic decomposition of HCOOH to produce H_2 [34], beneficial to the catalytic reduction of nitrate.

Table 1 summarizes the Pd/Ag (or Pd/Cu) molar ratios in the reaction system and in the obtained catalysts analyzed by ICP-OES. The Pd/Ag (or Pd/Cu) molar ratios in the obtained catalysts was close to that in the reaction system, which clearly demonstrated that the controlled surface reaction process was an efficient process to load Ag (or Cu) onto $\text{Pd}/\text{SiO}_2\text{-NH}_2$ catalyst. To examine the specific surface area and pore structure of these $\text{PdAg}/\text{SiO}_2\text{-NH}_2$

Table 1

Pd/Ag (or Pd/Cu) molar ratios in the reaction system and in the obtained catalysts analyzed by ICP-OES.

Catalyst	Initial molar ratio	Pd:M(wt%)	Real molar ratio
Pd:Ag	1:1	0.9829:0.8802	1:0.89
Pd:Ag	1:0.5	0.9713:0.4542	1:0.46
Pd:Ag	1:0.25	0.9564:0.2206	1:0.23
Pd:Cu	1:0.5	0.9352:0.2259	1:0.41

NH_2 catalysts, N_2 adsorption/desorption isotherm measurements were conducted, and the results were summarized in **Table 2**. The surface modification of $-\text{NH}_2$ on SiO_2 catalyst support and the subsequent loading of PdAg alloy nanoparticles only had moderate

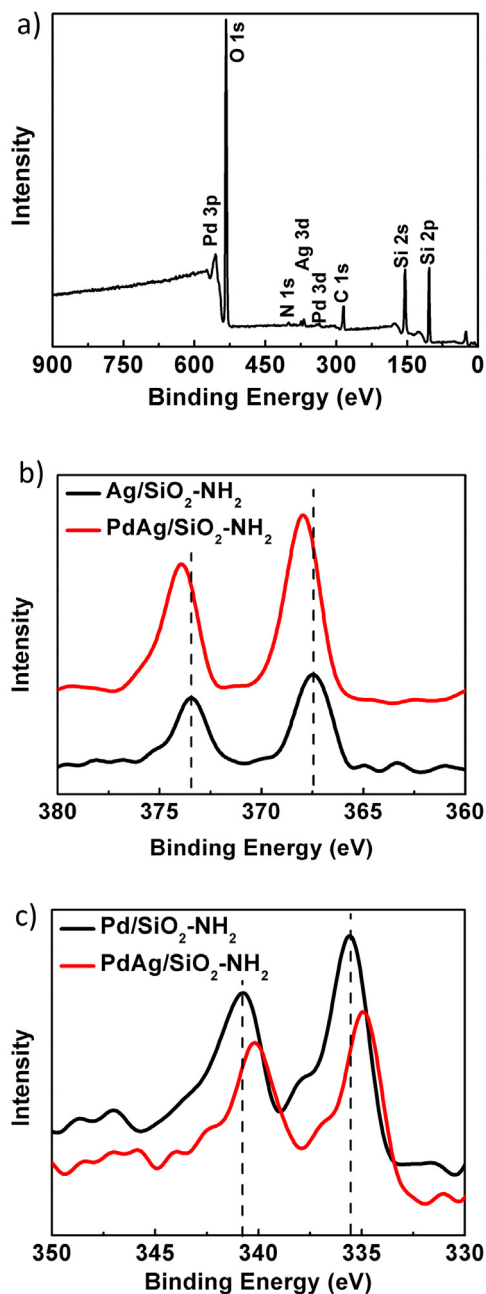


Fig. 2. (a) The representative survey XPS spectrum of PdAg1:0.5/SiO₂-NH₂ catalyst. (b) The high-resolution XPS scans over Ag 3d peaks of PdAg1:0.5/SiO₂-NH₂ catalyst and Ag0.5 wt% /SiO₂-NH₂ catalyst. (c) The high-resolution XPS scans over Pd 3d peaks of PdAg1:0.5/SiO₂-NH₂ catalyst and Pd1 wt% /SiO₂-NH₂ catalyst.

Table 2

BET specific surface area, average pore size, and specific pore volume of SiO₂ support, SiO₂-NH₂ support, and PdAg/SiO₂-NH₂ catalysts.

Sample	BET Specific Surface Area (m ² /g)	Specific Pore Volume (cm ³ /g)
SiO ₂	344	0.938
SiO ₂ -NH ₂	323	0.888
PdAg1:0.25/SiO ₂ -NH ₂	318	0.862
PdAg1:0.5/SiO ₂ -NH ₂	308	0.849
PdAg1:1/SiO ₂ -NH ₂	310	0.853
PdCu1:0.5/SiO ₂ -NH ₂	309	0.857

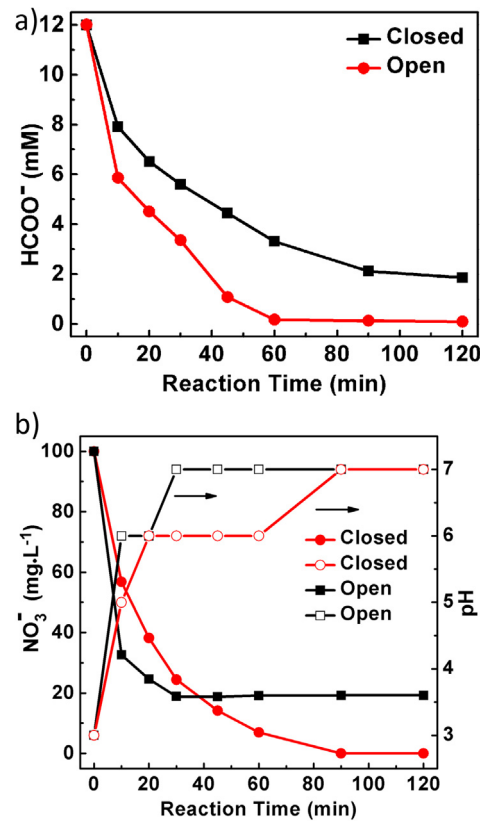


Fig. 3. (a) The catalytic HCOOH decomposition and (b) the catalytic nitrate reduction performances of the PdAg1:0.5/SiO₂-NH₂ catalyst and solution pH change in an open and a closed reaction system, respectively.

effects on its specific surface area and pore volume. PdAg/SiO₂-NH₂ catalysts still had a high specific area of ~310 to 318 m²/g and pore volume of ~0.849 to 0.862 cm³/g, which were beneficial for their efficient contact with HCOOH/NO₃⁻ in water and subsequent catalytic nitrate reduction performance.

3.2. Effect of open and closed reaction systems on the catalytic nitrate reduction performance of PdAg/SiO₂-NH₂ catalyst

The reaction system of open or closed design could largely affect the reaction if gaseous reactants or products are involved in the reaction, while few researches had investigated its influence on the catalytic nitrate reduction. Fig. 3a shows the catalytic HCOOH decomposition performances of the PdAg1:0.5/SiO₂-NH₂ catalyst in an open and a closed reaction system, respectively. It demonstrated clearly that the catalytic HCOOH decomposition was much faster in the open reaction system than in the closed system by the same catalyst. This comparison result was easy to understand because the gaseous catalytic HCOOH decomposition products as H₂ and CO₂ could easily escape from the solution in the open reaction system which facilitates the further catalytic HCOOH decomposition, while in the closed reaction system the escape of H₂ and CO₂ was more difficult because the escape of H₂ and CO₂ increased the pressure in the head space of the reactor and could hinder the further escape of H₂ and CO₂.

Fig. 3b shows the catalytic nitrate reduction performances of the PdAg1:0.5/SiO₂-NH₂ catalyst in an open and a closed reaction system, respectively, and the solution pH for both systems were also presented. In the open reaction system, the initial nitrate reduction rate was faster, but it slowed down quickly. The nitrate reduction rate decreased with the increase of solution pH [12,30,32]. When

the pH reached ~ 7 , the nitrate reduction mostly stopped. After only ~ 30 min, the reaction stopped and the residual nitrate ratio was $\sim 20\%$. In the closed reaction system, however, the nitrate concentration continued to drop until a complete removal at ~ 90 min. In the open system, more H_2 and CO_2 produced by the faster HCOOH decomposition could participate in the beginning stage of the catalytic nitrate reduction, resulted in a faster nitrate reduction rate than that in the closed reaction system. As time went by, however, the escape of produced CO_2 in the open reaction system could cause a quick increase of the solution pH due to the loss of solution pH buffer and subsequently hinder the catalytic nitrate reduction [12,30,32], while the escape of produced H_2 could also result in its insufficient utilization. In the closed reaction system, the loss of produced H_2 and CO_2 was much less than that in the open reaction system, so the catalytic nitrate reduction could continue until its complete reduction. Thus, the closed reaction system was used in the following sections.

3.3. Catalytic nitrate reduction performance comparison between $\text{PdAg/SiO}_2\text{-NH}_2$ and PdAg/SiO_2 catalysts

For the catalytic reduction with HCOOH as the reducing agent precursor, previous studies had demonstrated that surface modification with amine groups could increase the HCOOH decomposition efficiency because it facilitated the rupture of O–H bond in HCOOH [48,49], which then enhanced the catalytic reduction efficiency of Cr(VI) [38]. Furthermore, amine groups on SiO_2 catalyst support were beneficial to prevent the agglomeration of Pd nanoparticles [49]. Thus, surface modification of SiO_2 catalyst support by $-\text{NH}_2$ was first introduced in the development of efficient catalyst for nitrate reduction with HCOOH as the reducing agent precursor. Fig. 4a shows the catalytic HCOOH decomposition performance comparison between the $\text{PdAg/SiO}_2\text{-NH}_2$ and PdAg/SiO_2 catalysts (Pd:Ag at 1:0.5). Both catalysts demonstrated a continuous catalytic decomposition effect on HCOOH , while the HCOOH decomposition speed by the $\text{PdAg1:0.5/SiO}_2\text{-NH}_2$ catalyst with the surface $-\text{NH}_2$ modification was much faster than that by its counterpart without the surface $-\text{NH}_2$ modification. The initial HCOOH decomposition rate by the $\text{PdAg1:0.5/SiO}_2\text{-NH}_2$ catalyst was $\sim 12.25 \text{ mmol HCOO}^-/(\text{h g}_{\text{cat}})$, which was about 7 times as that by the PdAg1:0.5/SiO_2 catalyst ($\sim 1.68 \text{ mmol HCOO}^-/(\text{h g}_{\text{cat}})$). After 2 h reaction, the amount of HCOOH decomposed by the $\text{PdAg1:0.5/SiO}_2\text{-NH}_2$ catalyst was almost three times as that by the PdAg1:0.5/SiO_2 catalyst. Fig. 4b shows the catalytic nitrate reduction performance comparison between the $\text{PdAg1:0.5/SiO}_2\text{-NH}_2$ and PdAg1:0.5/SiO_2 catalysts. As expected, both catalysts demonstrated the catalytic reduction effect on nitrate, while the nitrate concentration dropped much faster by the $\text{PdAg1:0.5/SiO}_2\text{-NH}_2$ catalyst than by the PdAg1:0.5/SiO_2 catalyst. The initial nitrate reduction rate by the $\text{PdAg1:0.5/SiO}_2\text{-NH}_2$ catalyst was $\sim 129.56 \text{ mg NO}_3^-/(\text{h g}_{\text{cat}})$, which was about 17 times as that by the PdAg1:0.5/SiO_2 catalyst ($\sim 7.62 \text{ mg NO}_3^-/(\text{h g}_{\text{cat}})$). Only after 90 min, no nitrate was detected in the treated solution by the $\text{PdAg1:0.5/SiO}_2\text{-NH}_2$ catalyst, while the nitrate concentration dropped just $\sim 30\%$ with the same treatment time by the PdAg1:0.5/SiO_2 catalyst. Thus, the introduction of surface $-\text{NH}_2$ modification on the catalyst was effective to enhance the nitrate reduction efficiency with HCOOH as the reducing agent precursor.

3.4. Catalytic nitrate reduction performance comparison between $\text{PdAg/SiO}_2\text{-NH}_2$ and $\text{PdCu/SiO}_2\text{-NH}_2$ catalysts

In previous catalytic nitrate reduction studies with H_2 as the reducing agent, the most examined promoter component was Cu [19], and it also demonstrated its effectiveness with HCOOH as the reducing agent precursor [31]. Thus, the catalytic nitrate reduc-

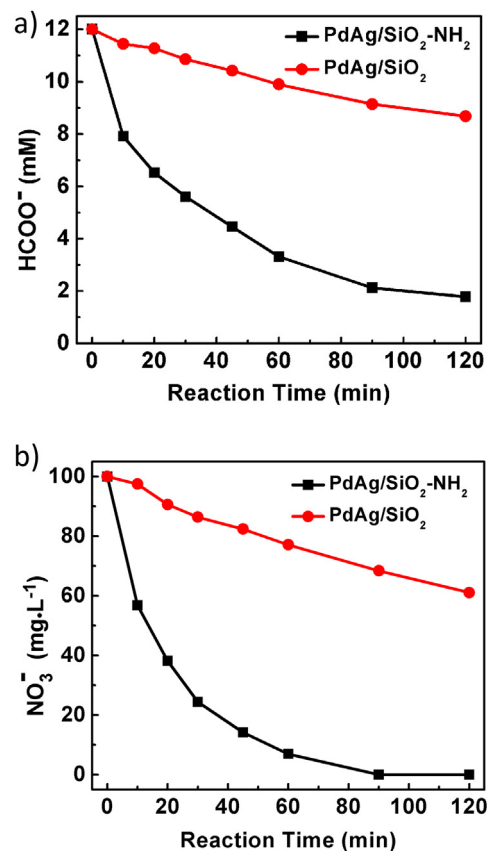


Fig. 4. (a) The catalytic HCOOH decomposition and (b) the catalytic nitrate reduction performance comparison between the $\text{PdAg/SiO}_2\text{-NH}_2$ and PdAg/SiO_2 catalysts (Pd:Ag at 1:0.5), respectively.

tion performance of our $\text{PdAg/SiO}_2\text{-NH}_2$ catalyst was compared with that of $\text{PdCu/SiO}_2\text{-NH}_2$ catalyst, and both of them had the surface $-\text{NH}_2$ modification. Fig. 5a shows the catalytic HCOOH decomposition performance comparison between the $\text{PdAg/SiO}_2\text{-NH}_2$ and $\text{PdCu/SiO}_2\text{-NH}_2$ catalysts with the same catalyst loading (Pd:Ag and Pd:Cu both at 1:0.5). Both catalysts demonstrated a continuous catalytic decomposition effect on HCOOH , while the HCOOH decomposition speed by the $\text{PdAg1:0.5/SiO}_2\text{-NH}_2$ catalyst was much faster than that by the $\text{PdCu1:0.5/SiO}_2\text{-NH}_2$ catalyst. After 2 h reaction, the amount of HCOOH decomposed by the $\text{PdAg1:0.5/SiO}_2\text{-NH}_2$ catalyst was about twice of that by the $\text{PdCu1:0.5/SiO}_2\text{-NH}_2$ catalyst. This comparison result was consistent with the work reported by Tedsree et al. on the catalytic HCOOH decomposition by a series of Pd@M (M: Ag, Au, Ru, Rh, Pt) core-shell nanocatalysts [34]. When two metals with different work functions contact, electrons could transfer from the one with a smaller work function to the other with the larger work function [34]. So it would be easier for electrons to transfer from Ag (work function at $\sim 4.26 \text{ eV}$) to Pd (work function at $\sim 5.12 \text{ eV}$) than from Cu (work function at $\sim 4.65 \text{ eV}$) to Pd, which was beneficial for the catalytic HCOOH decomposition [50,34]. Thus, the catalytic nitrate reduction should be more efficient by $\text{PdAg/SiO}_2\text{-NH}_2$ catalyst than by $\text{PdCu/SiO}_2\text{-NH}_2$ catalyst because of its more efficient HCOOH decomposition.

The catalytic nitrate reduction performance comparison between the $\text{PdAg1:0.5/SiO}_2\text{-NH}_2$ catalyst and the $\text{PdCu1:0.5/SiO}_2\text{-NH}_2$ catalyst clearly verified this deduction. Fig. 5b shows the catalytic nitrate reduction performance comparison between the $\text{PdAg1:0.5/SiO}_2\text{-NH}_2$ and $\text{PdCu1:0.5/SiO}_2\text{-NH}_2$ catalysts. Both catalysts demonstrated the catalytic reduction effect on nitrate,

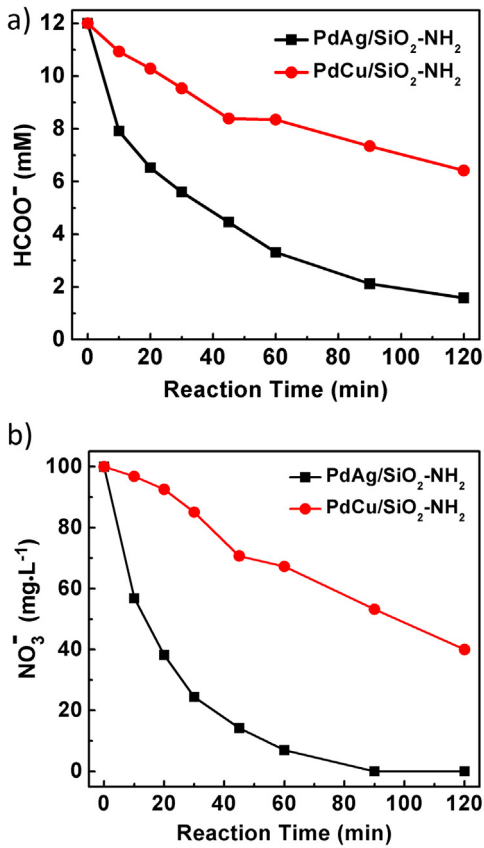


Fig. 5. (a) The catalytic HCOOH decomposition and (b) the catalytic nitrate reduction performance comparison between the PdAg/SiO₂-NH₂ and PdCu/SiO₂-NH₂ catalysts with the same catalyst loading (Pd:Ag and Pd:Cu both at 1:0.5), respectively.

while the nitrate concentration dropped much faster by the PdAg1:0.5/SiO₂-NH₂ catalyst than by the PdCu1:0.5/SiO₂-NH₂ catalyst. Only after 90 min, no nitrate was detected in the treated solution by the PdAg1:0.5/SiO₂-NH₂ catalyst, while the nitrate concentration dropped less than 50% with the same treatment time by the PdCu1:0.5/SiO₂-NH₂ catalyst. Thus, a superior nitrate reduction catalyst of PdAg/SiO₂-NH₂ was developed, which could effectively reduce nitrate with HCOOH as the reducing agent precursor. Besides the HCOOH decomposition effect, electronic effect, lattice strain and the overall binding strength of possible reactants/intermediates could also affect the nitrate removal performance of these catalysts, which needs further study to investigate.

3.5. Effect of Pd/Ag ratio on the catalytic nitrate reduction performance of PdAg/SiO₂-NH₂ catalyst

The Pd/Ag ratio in PdAg alloy nanoparticles could largely affect the nitrate reduction performance of the PdAg/SiO₂-NH₂ catalyst. Samples with a series of Pd/Ag atomic ratios of 1:1, 1:0.5, 1:0.25, and 1:0 were examined for their catalytic HCOOH decomposition and nitrate reduction performances. Fig. 6a shows the catalytic HCOOH decomposition performance comparison between these PdAg/SiO₂-NH₂ catalysts and Pd/SiO₂-NH₂ catalyst without Ag loading. It demonstrated clearly that the loading of Ag could largely enhance the HCOOH decomposition, especially with the increase of the reaction time. With the further increase of the Ag amount (over 1:0.25), the HCOOH decomposition rate gradually decreased. The loading of Ag to form PdAg alloy nanoparticles could have two major impacts on the catalytic decomposition of HCOOH. On the one hand, the electron transfer Ag to Pd was beneficial for the

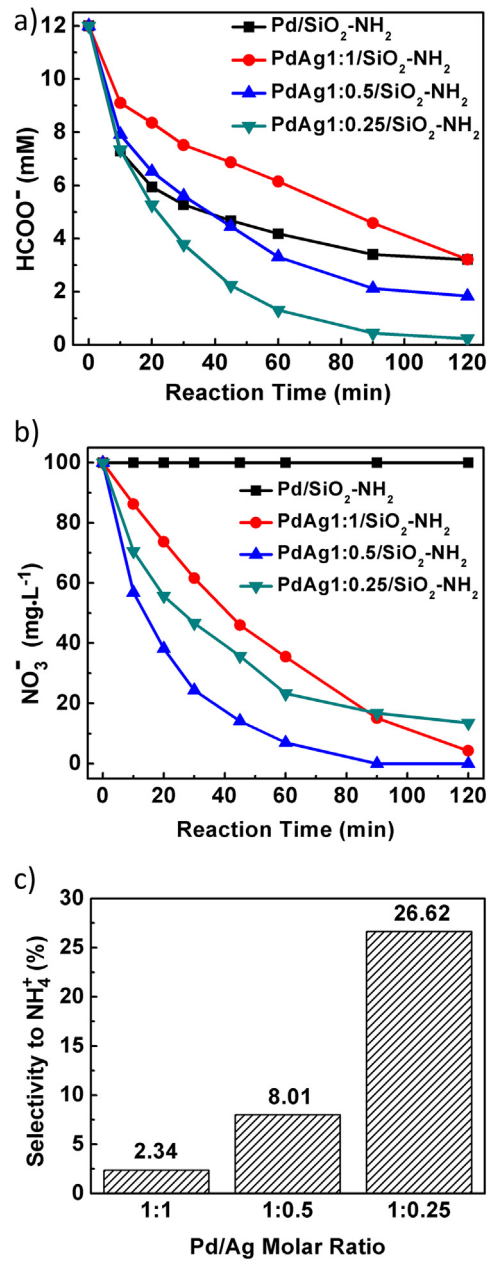


Fig. 6. (a) The catalytic HCOOH decomposition and (b) the catalytic nitrate reduction performance comparison between PdAg/SiO₂-NH₂ catalysts and Pd/SiO₂-NH₂ catalyst without Ag loading, respectively. (c) The selectivity to undesirable product of NH₄⁺ by PdAg/SiO₂-NH₂ catalysts with the same nitrate conversion percentage of ~75% to meet its drinking water standard recommended by the World Health Organization at 25 mg/L.

catalytic HCOOH decomposition [34]; on the other hand, Ag could occupy part of active sites and subsequently result in the decrease of adsorption/decomposition of HCOOH [51]. Thus, an optimal Ag content existed for these PdAg/SiO₂-NH₂ catalysts for the catalytic HCOOH decomposition.

Fig. 6b shows the catalytic nitrate reduction performance comparison between these PdAg/SiO₂-NH₂ catalysts and Pd/SiO₂-NH₂ catalyst without Ag loading. As expected, no nitrate reduction could be observed by Pd/SiO₂-NH₂ catalyst because the catalytic nitrate reduction required a promoter to reduce nitrate to nitrite firstly to start this process. PdAg/SiO₂-NH₂ catalysts, however, all demonstrated a continuous catalytic decomposition effect on nitrate, in which Ag served as the promoter to reduce nitrate to nitrite

and nitrite was further reduced by Pd [34]. Interestingly, it was found that the catalytic nitrate reduction efficiency ranking of these PdAg/SiO₂-NH₂ catalysts was different from their catalytic HCOOH decomposition efficiency ranking. Although the PdAg1:0.25/SiO₂-NH₂ catalyst was found to possess the best catalytic HCOOH decomposition efficiency, the PdAg1:0.5/SiO₂-NH₂ catalyst, however, demonstrated the best catalytic nitrate reduction efficiency among them. After ~90 min treatment, no nitrate could be detected in the solution treated by the PdAg1:0.5/SiO₂-NH₂ catalyst. For the PdAg1:0.25/SiO₂-NH₂ and PdAg1:1/SiO₂-NH₂ catalysts, the catalytic nitrate reduction by the PdAg1:0.25/SiO₂-NH₂ catalyst was faster at first than that by the PdAg1:1/SiO₂-NH₂ catalyst, but it gradually slowed down with the increase of the reaction time. After ~80 min treatment, more nitrate was catalytically reduced by the PdAg1:1/SiO₂-NH₂ catalyst than by the PdAg1:0.25/SiO₂-NH₂ catalyst, although the catalytic HCOOH decomposition by the PdAg1:0.25/SiO₂-NH₂ catalyst was always higher than that by the PdAg1:1/SiO₂-NH₂ catalyst.

The observed different rankings of these PdAg/SiO₂-NH₂ catalysts on their catalytic HCOOH decomposition and nitrate reduction efficiencies could be attributed to two major factors. On the one hand, Ag served as the promoter in these PdAg/SiO₂-NH₂ catalysts to reduce nitrate to nitrite, while nitrite was further reduced on Pd by reducing agents. Thus, the amount of Ag in PdAg alloy nanoparticles should be enough so coordinated catalytic reductions of nitrate and nitrite could happen to have the optimized nitrate removal performance. On the other hand, the HCOOH decomposition speed should be moderate to allow the nitrite reduction on Pd to make the full use of the reducing agent. If the HCOOH decomposition speed was too fast, large parts of the produced hydrogen and CO₂ could be wasted due to their volatilization. Thus, fewer HCOOH could be left in the solution for the catalytic nitrate reduction. If the HCOOH decomposition speed was too slow, there might not be enough hydrogen and CO₂ produced to serve as the reducing agent and buffer, respectively, which could also result in a poor nitrate removal performance. Thus, an optimized Pd/Ag ratio in PdAg alloy nanoparticles existed for the nitrate removal performance, which was not the same as the optimized Pd/Ag ratio for the HCOOH decomposition performance.

Fig. 6c compares the selectivity to undesirable product of NH₄⁺ by these PdAg/SiO₂-NH₂ catalysts with the same nitrate conversion percentage of ~75% to meet its drinking water standard recommended by the World Health Organization at 25 mg/L. It was found that the selectivity to NH₄⁺ increased with the decrease of Pd/Ag ratio. When the Pd/Ag ratio was 1:1, the selectivity to NH₄⁺ was only ~2.34%, while it increased to ~8.01% and 26.62% when the Pd/Ag ratio was 1:0.5 and 1:0.25, respectively. It had been found that the solution pH had a large impact on the product selectivity of catalytic nitrate reduction, and the NH₄⁺ formation could increase with the increase of the solution pH [52]. When the PdAg1:0.25/SiO₂-NH₂ was used, the fast decomposition of HCOOH could increase the solution pH more quickly than PdAg1:0.5/SiO₂-NH₂ and PdAg1:1/SiO₂-NH₂ catalysts (see Table S1 in the Supplementary material), which was in favor of the NH₄⁺ formation. Furthermore, active centers of Pd at different regions could have different reducing capacities as Yoshinaga et al. previously reported [53]. It had been found that the hydrogenation capacity of Pd active centers located at corners and edges of Pd nanocrystals was higher than that of Pd active centers located at terraces of Pd nanocrystals. Thus, nitrite tended to be reduced to NH₄⁺ at Pd active centers located at corners and edges of Pd nanocrystals by the deep hydrogenation. As loaded by the controlled surface reaction method, Ag preferred to be loaded at the corners and edges of Pd nanocrystals first. Thus, with the increase of Ag loading, more sites at the corners and edges of Pd nanocrystals could be occupied by Ag, which resulted in the decreased selectivity to NH₄⁺ [54]. Both

factors contributed to the increased selectivity to NH₄⁺ with the decrease of Pd/Ag ratio.

4. Conclusions

In summary, a PdAg/SiO₂-NH₂ catalyst was developed, which demonstrated an effective catalytic nitrate reduction performance with HCOOH as the reducing agent precursor for the first time. The surface -NH₂ modification of SiO₂ catalyst support largely enhanced its catalytic nitrate reduction performance because it could facilitate the rupture of O-H bond in HCOOH. PdAg alloy nanoparticles were superior to PdCu alloy nanoparticles as the catalyst for the nitrate reduction with HCOOH as the reducing agent precursor, which could be attributed to the better electron transfer from Ag to Pd than from Cu to Pd due to the larger difference of work function between Pd and Ag, beneficial for the catalytic HCOOH decomposition. An optimized Pd:Ag molar ratio (1:0.5) in PdAg alloy nanoparticles existed for the nitrate reduction, which was found to be different from the optimized Pd:Ag molar ratio (1:0.25) for the HCOOH decomposition.

Acknowledgements

This study was supported by the Basic Science Innovation Program of Shenyang National Laboratory for Materials Science (Grant No. Y4N56R1161 and Y4N56F2161), and the National Natural Science Foundation of China (Grant No. 51502305).

Appendix A. Supplementary data

Supplementary data associated with this article can be found, in the online version, at <http://dx.doi.org/10.1016/j.apcatb.2016.10.048>.

References

- [1] J.P. Van der Hoek, W.K. Van der Hoek, A. Klapwijk, *Water Air Soil Pollut.* 37 (1988) 41–53.
- [2] L.W. Canter, *Nitrates in Groundwater*, CRC Press, Boca Raton, FL, 1996.
- [3] D.M. Freedman, K.P. Cantor, M.H. Ward, K.J. Helzlsouer, *Arch. Environ. Health* 55 (2000) 326–329.
- [4] Drinking Water Directive 98/83/EC.
- [5] L. Bontoux, N. Bournis, D. Papameletiou, *IPTS Rep.* 6 (1996) 7.
- [6] D.A. Andrews, C. Harward, *J. Inst. Water Environ. Manage.* 8 (1994) 120–127.
- [7] O.K. Marquardt, *Aqua* 1 (1987) 39–44.
- [8] R. Rautenbach, W. Kopp, G. Van Opbergen, R. Hellekes, *Desalination* 65 (1987) 241–258.
- [9] F. Zhang, R. Jin, J. Chen, C. Shao, W. Gao, L. Li, N. Guan, *J. Catal.* 232 (2005) 424–431.
- [10] F. Epron, F. Gauthard, C. Pinéda, J. Barbier, *J. Catal.* 206 (2002) 363–367.
- [11] V. Mateju, S. Cizinska, J. Krejci, T. Janoch, *Enzyme Microbiol. Technol.* 14 (1992) 170–183.
- [12] N. Barrabés, J. Sá, *Appl. Catal. B: Environ.* 104 (2011) 1–5.
- [13] U. Prütse, K.D. Vorlop, *J. Mol. Catal. A: Chem.* 173 (2001) 313–328.
- [14] K.D. Vorlop, T. Tacke, *Chem. Ing. Tech.* 61 (1989) 836–837.
- [15] A. Pintar, J. Batista, *Catal. Today* 53 (1999) 35–50.
- [16] H. Berndt, I. Mönnich, B. Lücke, M. Menzel, *Appl. Cat. B: Environ.* 30 (2001) 111–122.
- [17] F. Epron, F. Gauthard, C. Pinéda, J. Barbier, *J. Catal.* 198 (2001) 309–318.
- [18] A. Palomares, *J. Catal.* 221 (2004) 62–66.
- [19] N. Barrabés, J. Just, A. Dafinov, F. Medina, J. Fierro, J. Sueiras, P. Salagre, Y. Cesteros, *Appl. Catal. B: Environ.* 62 (2006) 77–85.
- [20] O.S.G.P. Soares, J.J.M. Órfão, M.F.R. Pereira, *Desalination* 279 (2011) 367–374.
- [21] S. Hamid, M.A. Kumar, W. Lee, *Appl. Catal. B: Environ.* 187 (2016) 37–46.
- [22] A. Garron, F. Epron, *Water Res.* 39 (2005) 3073–3081.
- [23] M. Grasemann, G. Laurenczy, *Energy Environ. Sci.* 5 (2012) 8171–8181.
- [24] D.A. Bulushev, S. Beloshapkin, J.R.H. Ross, *Catal. Today* 154 (2010) 7–12.
- [25] Y.L. Qin, J. Wang, F.Z. Meng, L.M. Wang, X.B. Zhang, *Chem. Commun.* 49 (2013) 10028–10030.
- [26] K. Jiang, K. Xu, S.Z. Zou, W.B. Cai, *J. Am. Chem. Soc.* 136 (2014) 4861–4864.
- [27] K. Jiang, H.X. Zhang, S.Z. Zou, W.B. Cai, *Phys. Chem. Chem. Phys.* 16 (2014) 20360–20376.
- [28] M. Ojeda, E. Iglesia, *Angew. Chem. Int. Ed.* 48 (2009) 4800–4803.
- [29] M.A. Omole, I.O. Owino, O.A. Sadik, *Appl. Cat. B: Environ.* 76 (2007) 158–167.
- [30] U. Prütse, M. Hähnlein, J. Daum, K.D. Vorlop, *Catal. Today* 55 (2000) 79–90.

[31] E.K. Choi, K.H. Park, H.B. Lee, M. Cho, S. Ahn, *J. Environ. Sci.* 25 (2013) 1696–1702.

[32] Y.N. Guo, J.H. Cheng, Y.Y. Hu, D.H. Li, *Appl. Catal. B: Environ.* 125 (2012) 21–27.

[33] F. Gauthard, F. Epron, J. Barbier, *J. Catal.* 220 (2003) 182–191.

[34] K. Tedsree, T. Li, S. Jones, C.W. Chan, K.M. Yu, P.A. Bagot, E.A. Marquis, G.D. Smith, S.C. Tsang, *Nat. Nanotechnol.* 6 (2011) 302–307.

[35] K. Jiang, H.X. Zhang, Y.Y. Yang, R. Mothes, H. Lang, W.B. Cai, *Chem. Commun.* 47 (2011) 11924–11926.

[36] A. Bulut, M. Yurderi, Y. Karatas, M. Zahmakiran, H. Kivrak, M. Gulcan, M. Kaya, *Appl. Cat. B: Environ.* 164 (2015) 324–333.

[37] Y. Karatas, A. Bulut, M. Yurderi, I.E. Ertas, O. Alal, M. Gulcan, M. Celebi, H. Kivrak, M. Kaya, M. Zahmakiran, *Appl. Catal. B: Environ.* 180 (2016) 586–595.

[38] M. Celebi, M. Yurderi, A. Bulut, M. Kaya, M. Zahmakiran, *Appl. Catal. B: Environ.* 180 (2016) 53–64.

[39] M. Yadav, T. Akita, N. Tsumori, Q. Xu, *J. Mater. Chem.* 22 (2012) 12582–12586.

[40] F.Z. Song, Q.L. Zhu, N. Tsumori, Q. Xu, *ACS Catal.* 5 (2015) 5141–5144.

[41] R.J. White, R. Luque, V.L. Budarin, J.H. Clarka, D.J. Macquarrie, *Chem. Soc. Rev.* 38 (2009) 481–494.

[42] A. Devadas, S. Vasudevan, F. Epron, *J. Hazard. Mater.* 185 (2011) 1412–1417.

[43] I. Taylor, A.G. Howard, *Anal. Chim. Acta* 271 (1993) 77–82.

[44] H.M. Dai, B.Q. Xia, L. Wen, C. Du, J. Su, W. Luo, G.Z. Cheng, *Appl. Catal. B: Environ.* 165 (2015) 57–62.

[45] S. Zhang, O. Metin, D. Su, S. Sun, *Angew. Chem. Int. Ed.* 52 (2013) 3681–3684.

[46] A. Bulut, M. Yurderi, Y. Karatas, Z. Say, H. Kivrak, M. Kaya, M. Gulcan, E. Ozensoy, M. Zahmakiran, *ACS Catal.* 5 (2015) 6099–6110.

[47] Z.L. Wang, J.M. Yan, Y. Ping, H.L. Wang, W.T. Zheng, Q. Jiang, *Angew. Chem. Int. Ed.* 52 (2013) 4406–4409.

[48] L.L. Wei, R. Gu, J.M. Lee, *Appl. Catal. B: Environ.* 176–177 (2015) 325–330.

[49] M. Martis, K. Mori, K. Fujiwara, W.S. Ahn, H. Yamashita, *J. Phys. Chem. C* 117 (2013) 2805–22810.

[50] H.B. Michaelson, *J. Appl. Phys.* 48 (1977) 4729–4733.

[51] X.J. Gu, Z.H. Lu, H.L. Jiang, T. Akita, Q. Xu, *J. Am. Chem. Soc.* 133 (2011) 11822–11825.

[52] L. Lemaignena, C. Tong, V. Begonb, R. Burchb, D. Chadwicka, *Catal. Today* 75 (2002) 43–48.

[53] Y. Yoshinaga, T. Akita, I. Mikami, T. Okuhara, *J. Catal.* 207 (2002) 37–45.

[54] R. Melendrez, G. Del Angel, V. Bertin, M.A. Valenzuela, J. Barbier, *J. Mol. Catal. A: Chem.* 157 (2000) 143–149.